

화장용 기름 종이로 이용하기 위한 폴리에틸렌옥사이드 나노섬유 쉬트의 기름 흡수능력 평가

윤옥자[†]

중앙대학교 신기능이미징연구소

(2016년 7월 19일 접수, 2016년 9월 8일 수정, 2016년 9월 29일 채택)

Oil Absorption Capacity of Polyethylene Oxide Nanofiber Sheets for Oil Blotting Cosmetic Sheets

Ok Ja Yoon[†]

Department of Physics, Institute of Innovative Functional Imaging, Chung-Ang University, Seoul 06974, Korea

(Received July 19, 2016; Revised September 8, 2016; Accepted September 29, 2016)

초록: 본 연구는 기존에 시판되고 있는 화장용 기름 흡수 쉬트 제품들과 비교하여 친환경적으로 분해성이 좋고 높은 표면적과 기름 흡수 능력을 가지는 제품 개발을 목적으로 하였다. 유기용매를 사용하지 않고 물에 잘 녹는 양친성 고분자인 폴리에틸렌 옥사이드(PEO)를 전기방사 방법을 이용하여 직경이 다른 두 종류의 나노섬유 쉬트를 개발하였고, 기름 흡수 및 보유 능력, 기름 흡수 후 광 투과성, 표면적, 열적 및 기계적 특성 평가를 수행하였다. 표면적이 높은 PEO 나노섬유 쉬트가 기존 제품과 비교하여 기름 흡수 능력이 11배 증가하였고 열적 및 기계적 특성 또한 향상됨을 확인하였다. 이러한 결과를 통하여 화장품 시장 및 의료 분야에 응용가능성을 확인하였다.

Abstract: Oil blotting cosmetic sheets are important products in the cosmetic and healthcare applications. However, they are limited by their relatively low oil absorption capacity due to their low surface area. In this study, I used an electrospinning method to develop two types of polyethylene oxide (PEO) nanofiber sheets with a large surface area. The properties of sheet, such as the change in the optical transmittance due to oil absorption, the oil absorption capacity, the oil retention capacity, the specific surface area, and thermal and mechanical properties, were evaluated. The oil absorption capacity of PEO nanofiber sheets (25 gauge) was found to be about 11 times greater than that of commercial oil blotting cosmetic sheets and the surface area, as well as the thermal and mechanical properties, increased slightly compared to PEO nanofiber sheets (21 gauge). PEO exhibit ideal characteristics of oil sorbent materials. Therefore, PEO nanofiber sheets with a high surface area are expected to exhibit greater oil absorption capacity than conventional oil blotting cosmetic sheets.

Keywords: polyethylene oxide, nanofiber sheets, oil absorption capacity, specific surface and porosity, oil blotting cosmetic sheets.

Introduction

Oil blotting films are widely used, before and after makeup application, to remove facial oil, in part to prevent skin diseases such as acne vulgaris.¹ Commercially available oil blotting products are typically made of synthetic polypropylene and polyurethane, plant-based papers, etc. The main characteristic of oil sorbent materials used for oil spill cleanup and oil

absorption is their hydrophobicity or oleophilicity.¹ In particular, polypropylene has a high oil sorption capacity because of its excellent hydrophobic-oleophilic property. Unfortunately, it exhibits a low level of biodegradability.^{1,2} A previous study reported the potential application of polyhydroxyalkanoates as cost-effective oil blotting films; however, the structural features of the developed materials with respect to the existing products were not discussed.³ Currently available commercial products are based on polymer films with a porous structure and do not feature structures with optimized surface areas. Various polymeric nanofibers, prepared by an electro-

[†]To whom correspondence should be addressed.

E-mail: yokk777@cau.ac.kr

©2016 The Polymer Society of Korea. All rights reserved.

spinning method, were evaluated for oil absorption and were found to exhibit an increased oil absorption capacity as a result of their high surface area to volume ratio.^{4,5} Moreover, a subtle regulation of micro- and nanostructures of electrospun polystyrene (PS) fibers was reported to form porous PS fibrous mats, which exhibited a higher oil absorption capacity than commercial materials.⁶

Polyethylene oxide (PEO) - containing amphiphilic block copolymers exhibit an interesting self-assembly properties involving both hydrophobic and hydrophilic segments.⁷ The hydrophobic sequences are generally based on styrene,⁸ dienes,⁹ or hydrogenated aliphatic polyolefin blocks.¹⁰ These amphiphiles are used in a wide range of applications, including polymeric surfactants,¹¹ the stabilization of dispersions,¹² the encapsulation of drugs,¹³ and the formulation of cosmetics.¹⁴ PEO exhibits some hydrophobic characteristics and forms thin monolayers at the air-water interface.¹⁵ Because of its characteristics such as biodegradability, water solubility, biocompatibility, and non-toxicity,¹⁶ it has been widely used in various biomedical engineering applications including protein adsorption inhibition,^{17,18} drug delivery systems,¹⁹ and the solid electrolytes in electrochemical devices.²⁰ A study of the structure of PEO nanofibers reported their mechanical and physical properties²¹; however, the oil absorption and retention properties of PEO nanofiber sheets have not yet been investigated.

In this study, I examined the oil absorption capacity of PEO nanofiber sheets, in comparison with the porous stretched polymer films used in existing commercial products. I developed PEO nanofiber sheets with a high surface area by using an electrospinning method with a 21 gauge and 25 gauge needles. To the best of our knowledge, PEO nanofiber sheets without any organic solvent have not yet been marketed as oil blotting cosmetic sheets. The oil blotting capacity of PEO nanofiber sheets was therefore examined from viewpoint of several important factors, namely, optical transmittance changes upon oil absorption, oil absorption capacity, oil retention capacity, the specific surface area and porosity due to diameter of nanofibers, and thermal and mechanical properties.

Experimental

Fabrication of PEO Nanofiber Sheets and Materials. A solution of PEO polymer with a viscosity molecular weight (M_v) of 400000 g·mol⁻¹ (Sigma Aldrich, USA) and a concentration of 8 wt% in distilled water (DW) was prepared and mixed by magnetic stirring for 5 h. The electrospun samples

were fabricated by electrospinning system (NanoNC, ESR 100 model, Korea). The electrospinning process was performed using the prepared solutions, which were placed in a 10 mL syringe fitted with a 21 gauge or 25 gauge needles. A syringe pump was used to supply the solution into the needle tip at a rate of 0.1 mL/h. A voltage of 13 kV was applied between the needle tip (anode) and the collecting plate (cathode) over a separation distance of 18 cm. As the PEO solution streamed through the electric field, the solvent evaporated and PEO nanofiber sheets were formed on the collecting plate. The PEO nanofiber sheets were cut into 2×2 cm squares, each with a thickness of 21.7±1.7 μm (N=5).

For comparison purposes, two existing commercial products were purchased from local supermarkets. Products A (Johnson & Johnson) and B (GATSBY) are polypropylene-based facial oil blotting films with a porous structure. Square samples of A and B, measuring 2×2 with a thickness of 21.6±0.75 and 36.2±0.79 μm (N=5), respectively, were prepared. The measured data are shown together with standard deviations.

Analysis of PEO Nanofiber Sheets. The morphology of PEO nanofiber sheets and the thickness of all the samples were measured using field emission scanning electron microscopy (FE-SEM) (JSM 7500F, JEOL Ltd., Japan). Optical images of oil absorbed samples were captured using a digital microscope (DIGIBIRD, OPT-200, Selectech Electronics Co., Ltd., China) with an accuracy in the μm range. The chemical properties of PEO nanofiber sheets were characterized by Fourier transform infrared spectroscopy (FTIR) (Nicolet 6700, Thermo Scientific, USA). The contact angle defining the hydrophilic and hydrophobic properties was measured using a Phoenix-300 Touch (Surface & Electro Optics Co. Ltd., Korea). DW and Bio-Oil (Union Swiss, South Africa) were automatically dropped the 6 μL droplets by a syringe pump onto the surface of all the samples. The contact angle was calculated by the software of Phoenix-300 Touch (Version 10.11, surface & Electro Optics Co. Ltd., Korea). The mechanical properties were measured using a dynamic mechanical analyzer (DMA) (SS6100, SEIKO Instruments, Japan) at room temperature and a rate of 150 mN/min. The specific surface area and pore size of all the samples were determined using a Brunauer–Emmett–Teller (BET) surface area analyzer (ASAP 2420, Micromeritics, USA). The nitrogen adsorption isotherms for each sample (1 g) were measured using an N₂ adsorption system at low temperature (77.35 K). The specific surface areas and pore size were determined using the BET method and the Barrett–Joyner–Halenda (BJH) model, respectively. A thermogravi-

metric analysis (TGA) was performed using a thermobalance (TG/DTA 7300, SEIKO Instruments, Japan) at a heating rate of 10 °C /min under nitrogen flow. The contact angle, BET, TGA values were all determined in duplicate.

The transmittance was measured using an ultraviolet-visible (UV-vis) spectrometer (Cary 5000 Varian, Agilent Technologies, USA) over a wavelength range 300-2500 nm, with a UV/vis resolution and near-infrared (NIR) of ≤ 0.03 nm and ≤ 0.2 nm, respectively. A commercial cosmetic oil (Bio-Oil, Union Swiss, South Africa) was used to measure the changes in the optical transparency upon oil absorption, as well as the oil absorption capacity, and oil retention capacity. The samples were measured ten times. The transmittance is expressed in terms of mean \pm standard deviation values. The student t-test was used to analyze the relationship between the different variables. A *p* value of less than 0.05 was considered to be statistically significant.

Determination of Transmittance, Oil Absorption Capacity, and Oil Retention Capacity. The transmittance was evaluated from the transparency changes of the square samples before and after oil treatment. Transparency changes were observed using a UV-vis spectrophotometer at the wavelength corresponding to the maximum absorbance for all samples.

For determine the oil absorption capacity, the samples were weighed prior to dipping into mineral oil. The samples were then immersed in mineral oil for 1 to 2 min, after which Kim-wipe tissues were used to remove any excess oil, and then the samples were weighed again to determine the amount of oil absorbed. The oil absorption capacity was calculated as follows²:

$$\text{Oil absorption capacity (g/g)} = \frac{\text{Sheet weight after dipping in oil} - \text{Initial sheet weight}}{\text{Initial sheet weight}} \quad (1)$$

After measuring the oil absorption capacity, the samples were wrapped in aluminum foil, placed under steel weight (1 Kg) for 1 to 2 min, and were then weighed again. The oil retention capacity was calculated as follows²:

$$\text{Oil retention capacity (\%)} = \left(1 - \frac{\text{Sheet weight after dipping in oil} - \text{Sheet weight after pressing}}{\text{Sheet weight after dipping in oil}}\right) \times 100 \quad (2)$$

Results and Discussion

Morphology and Characteristics of PEO Nanofiber Sheets. The two types of needle used during the electro-

spinning process for the preparation of PEO nanofiber sheets, namely, a 21 gauge and 25 gauge needles, have different diameters, specifically, 0.50 and 0.26 mm, respectively. Thus, the PEO nanofiber sheets produced with the 25 gauge needle have a slightly lower average diameter (0.59 ± 0.13 μm) relative to those made with 21 gauge needle (0.71 ± 0.13 μm) ($N=20$). As shown in Figure 1(a), (b), the PEO nanofiber sheets were exhibited a uniform distribution. Products A (blue color) and B (black color) are polypropylene-based facial oil blotting cosmetics consisting of a single film with micro-embossed structure (average diameters of 171 and 311 μm , respectively ($N=20$)) containing micro-pores for highly efficient oil absorption (data not shown). Because long-term stability is an important property for oil blotting cosmetic sheets, I investigated the time-dependent morphology change of nanofibers. Although a change was observed in the morphology of the PEO nanofiber sheets after three months, with bent and loose as illustrated Figure 1(c), (d), PEO nanofiber sheets offer long-term stability while also eco-friendly products. To determine the effect of oil absorption, optical images of the PEO nanofiber sheets and commercial products A and B were recorded before and after treatment with a few Bio-Oil drops (2 μL) (Figure 2). The effect of oil absorption on the samples could be observed by optical microscope after 1 to 2 min. All of the samples are shown in Figure 2(a). PEO nanofiber sheets exhibit a high level of absorption capacity and a rapid absorption rate (Figure 2(b), (c)) whereas slow absorption and spread were observed for products A and B (Figure 2(d), (e)). Moreover, the color

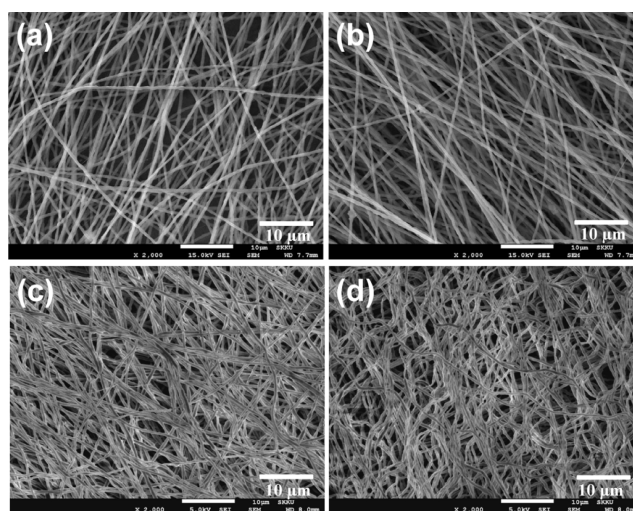


Figure 1. Morphologies of PEO nanofiber sheets fabricated using (a) a 21 gauge needle; (b) a 25 gauge needle; (c) a 21 gauge needle after three months; (d) a 25 gauge needle after three months.

changes of the films are very important, as they are representative of the oil absorption ability.

The FTIR spectra of PEO nanofiber sheets incorporate the following vibration bands: C-H stretching mode at 2880 cm^{-1} , CH_2 scissoring mode at 1470 cm^{-1} , CH_2 wagging mode at 1340 cm^{-1} , CH_2 twisting mode at 1240 and 1280 cm^{-1} , C-O-C stretching at 1100 cm^{-1} , C-O-C vibration at 962 cm^{-1} , and CH_2 rocking at 843 cm^{-1} (Figure 3).²² The presence of a hydrophilic head, suggested by the C-O-C stretching, and a hydrophobic tail, represented by the CH_2 group, confirmed the amphiphilic properties of the PEO chains.¹⁶

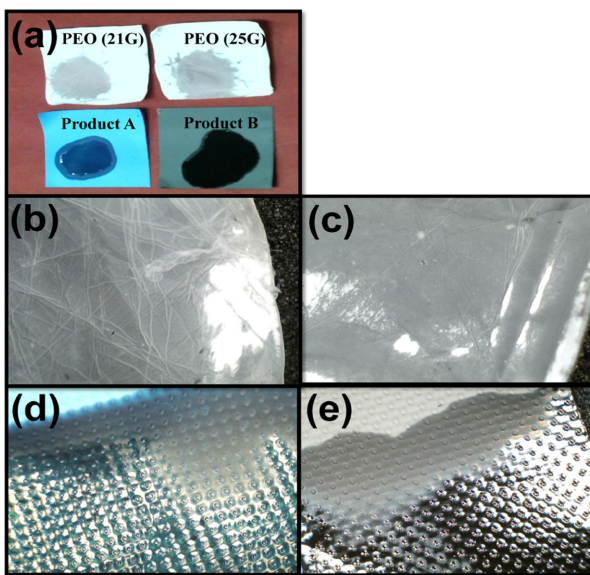


Figure 2. Optical images after oil treatment of (a) the PEO nanofiber sheets fabricated using a 21 gauge needle; (b) the PEO nanofiber sheets fabricated using a 25 gauge needle; (c) product A; (d) product B.

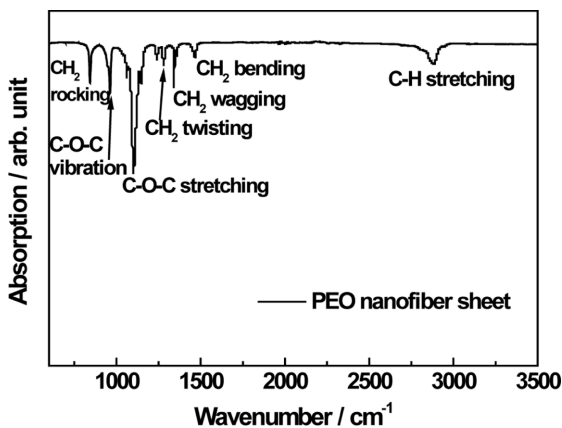


Figure 3. FTIR spectra of PEO nanofiber sheets.

The Figure 4 shows the hydrophilic and hydrophobic properties of all the samples. The contact angles of the PEO nanofiber sheets (21 gauge and 25 gauge) in Figure 4(a) change from 78.3° and 93° to 8.8° and 21.7° over 2 min, respectively. However, the samples of product A and B exhibited constant values from the initial value at 117.7° and 113.8° . The PEO nanofiber sheets were confirmed as exhibiting hydrophilic property while product samples exhibited hydrophobic property. The hydrophilicity of PEO nanofiber sheets (21 gauge) was slightly greater than that of PEO nanofiber sheets (25 gauge). The contact angles after Bio-Oil was dropped on the sheets, over 2 min, are shown in Figure 6(b). These results confirmed that the oil absorption of PEO nanofiber sheets (25 gauge) with a high surface area was greatly superior to that of the other samples.

The specific surface area and porous structure of all the samples were measured by BET. The results are listed in Table 1. The specific surface area of PEO nanofiber sheets (25 gauge), found to be $4.55\text{ (m}^2/\text{g)}$, is greater than those of the other samples. The total pore volumes of the electrospun samples were found to be the same, at $0.017\text{ (cm}^3/\text{g)}$, but this value was greater than that of product samples. The average pore size of PEO nanofiber sheets (25 gauge) was slightly smaller than that

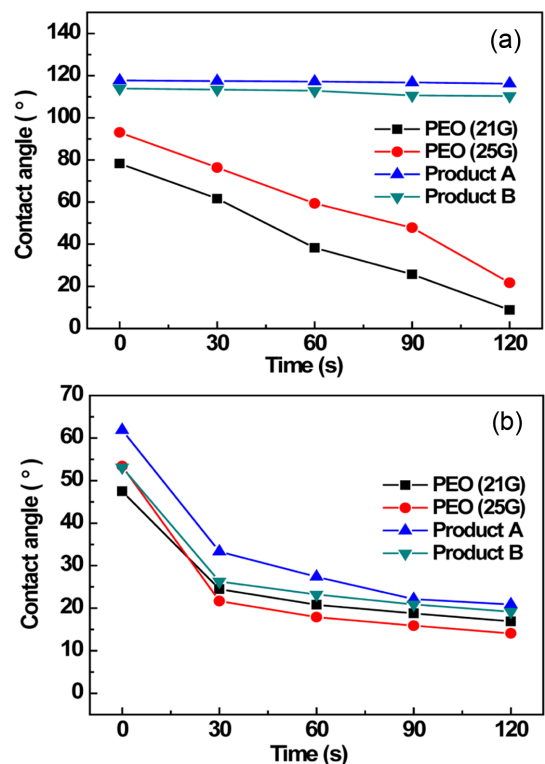
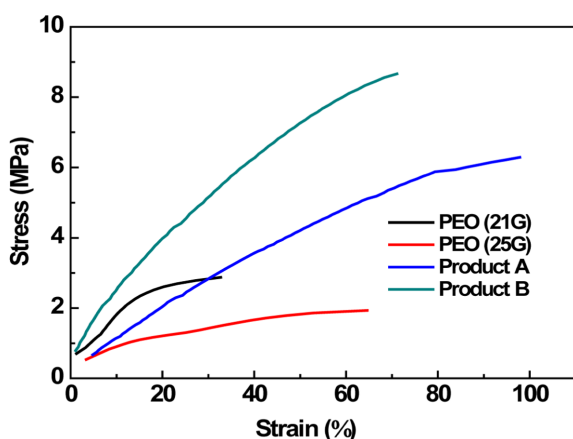


Figure 4. Contact angles by droplet of (a) DW; (b) bio-oil.

Table 1. Specific Surface Area, Total Pore Volume and Average Pore Size of PEO Nanofiber Sheets, Product A and Product B

Sample	Specific surface area (m ² /g)	Total pore volume (cm ³ /g)	Average pore size (nm)
PEO (21G)	4.34	0.017	16.25
PEO (25G)	4.55	0.017	15.31
Product A	1.01	0.002	7.15
Product B	2.00	0.006	12.87

**Figure 5.** Stress-strain curves of PEO nanofiber sheets (21 gauge and 25 gauge needles), and product samples (A and B).

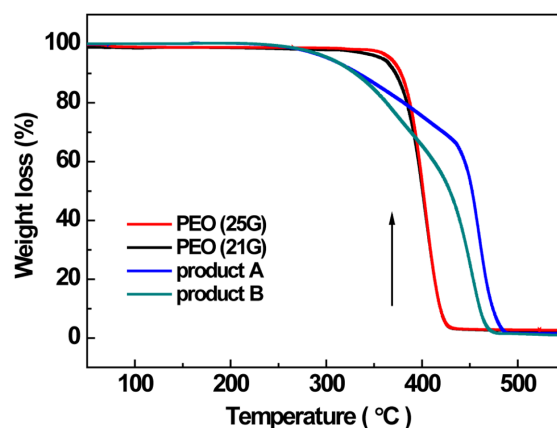
of PEO nanofiber sheets (21 gauge) because of the reduced diameters of nanofibers.

The mechanical properties of all the samples were obtained by DMA, as shown in Figure 5 and Table 2. The PEO nanofiber sheets (25 gauge) have the lowest tensile strength of all the samples. However, the tensile strain and modulus of PEO nanofiber sheets (25 gauge), with its high surface area, were much better than those of the other samples and were greater by 10% and a factor of 4, respectively, relative to PEO nanofiber sheets (21 gauge).

The thermomechanical properties of PEO nanofiber sheets were measured using thermogravimetric analysis (TGA) to determine the thermal stability. The TGA curves of electrospun samples produced with the 21 and 25 gauge needles, shown in Figure 6, are degraded by a single step at 355 and 368 °C, respectively and do not change over 430 °C. The degradation of PEO nanofiber sheets (25 gauge) increased slightly compared to PEO nanofiber sheets (21 gauge). The degradation temperatures of product A and B were detected at first step of 259 °C and product A exhibited a second step at 435 °C. The

Table 2. Mechanical Property of PEO Nanofiber Sheets, Product A and Product B

Sample	Tensile stress (MPa)	Tensile strain (%)	Tensile modulus (MPa)
PEO (21G)	3.02 (±0.08)	46.99 (±8.22)	14.05 (±2.32)
PEO (25G)	1.63 (±0.16)	56.64 (±14.82)	57.64 (±14.82)
Product A	5.54 (±0.41)	85.05 (±5.75)	15.39 (±0.44)
Product B	9.33 (±0.44)	73.93 (±2.08)	7.94 (±0.15)

**Figure 6.** TGA curves of PEO nanofiber sheets (21 gauge and 25 gauge needles), and product samples (A and B).

degradation temperatures of product samples were lower than those of PEO nanofiber sheets. This indicated that PEO nanofiber sheets with a high surface area exhibited improved thermal stability and this level of performance points to the applicability of PEO nanofiber sheets as practical cosmetic products.

Transmittance Changes of PEO Nanofiber Sheets. The transmittance of oil blotting cosmetic sheets is such that the degree of oil absorption corresponds to changes in the color of material.³ The density of PEO nanofiber sheets (21 gauge and 25 gauge) and products (A and B) was measured and found to be 5.43±0.70, 5.83±0.65, 1.41±0.02 and 0.9±0.01 (g/cm³), respectively. The transmittance changes of PEO nanofiber sheets were obtained from the transparency changes after oil treatment (Figure 7). Upon oil treatment, the transmittance of PEO nanofiber sheets (21 gauge) changed by a factor of 57, from 0.4±4.06 to 22.95±2.46 (%), whereas that of PEO nanofiber sheets (25 gauge) changed by a factor of 43, from 0.51±0.06 to 21.75±8.14 (%). The transmittance changes of PEO nanofiber sheets with the small diameter (25 gauge) were found to be lower than those of the PEO nanofiber sheets (21

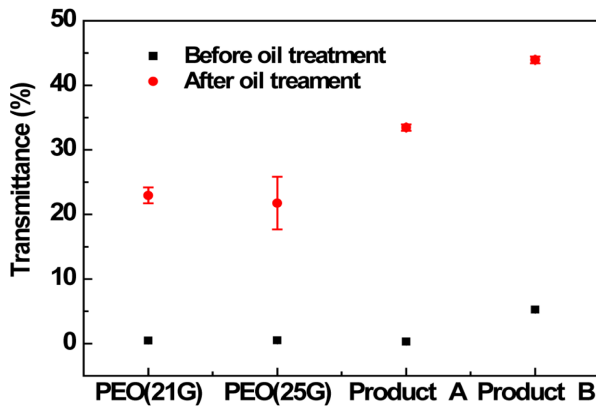


Figure 7. Transmittance of PEO nanofiber sheets and of products A and B, before and after oil treatment.

gauge), because of the higher density. On the other hand, the transmittance of product A changed by a factor of 107, from 0.31 ± 0.01 , to 33.44 ± 1.44 (%), while that of product B increased slightly by a factor of 8.33, from 5.27 ± 0.84 to 43.94 ± 1.68 (%).

The transmittance values of products A and B (blue and black, respectively) was affected by their original color. The transmittance after oil treatment was found to slightly decrease the opacity of PEO nanofiber sheets relative to that of products A and B. The results of the student t-test of transmittance values showed no significant difference in the relationship between all the samples: PEO nanofiber sheets (21 gauge) vs blue and black (t -value: 1.09, p -value: 0.30), PEO nanofiber sheets (25 gauge) vs blue and black (t -value: 0.59, p -value: 0.57).

Oil Absorption and Oil Retention Capacities of PEO Nanofiber Sheets. To evaluate the adequacy of the prepared samples as cosmetic oil blotting materials, their oil absorption and retention capacities were measured (Figure 8). The oil absorption capacity of PEO nanofiber sheets fabricated using 21 and 25 gauge needles is 3.2 ± 1.24 and 4.54 ± 1.45 (g/g), respectively, whereas similar values were found for products A and B with 0.4 ± 0.08 and 0.4 ± 0.06 (g/g), respectively. Thus, the oil absorption capacity of PEO nanofiber sheets is about 11 times greater than that of commercial products A and B (Figure 8(a)). Moreover, the higher oil absorption capacity of PEO nanofiber sheets (25 gauge) is due to their higher surface area relative to that of the nanofiber sheets (21 gauge). The oil retention capacity of PEO nanofiber sheets was measured to be within 99.2%, which is excellent relative to that of products A and B (within 98.4%) (Figure 8(b)).

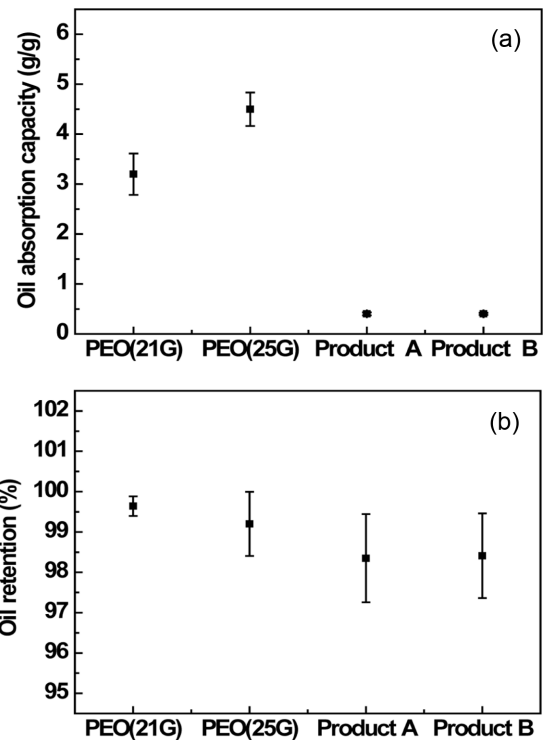


Figure 8. (a) Comparison of the oil absorption of PEO nanofiber sheets (21 gauge), PEO nanofiber sheets (25 gauge), product A, and product B; (b) Comparison of oil retention capacity of PEO nanofiber sheets (21 gauge), PEO nanofiber sheets (25 gauge), product A, and product B.

Conclusions

The oil blotting characteristics of PEO nanofiber sheets were investigated and compared to those of existing commercial products with porous stretched polymer films. Two types of PEO nanofiber sheets using 21 and 25 gauge needles were prepared by electrospinning method, and the adequacy of the prepared materials as cosmetic oil blotting sheets was investigated by evaluating the transmittance changes upon oil absorption, the oil absorption capacity, the oil retention capacity, the specific surface area and porosity due to diameter of nanofibers, and thermal and mechanical properties.

The contact angles by a drop of bio-oil over 2 min confirmed that the oil absorption of PEO nanofiber sheets (25 gauge) was excellent compare to those of the other samples. The specific surface area of PEO nanofiber sheets (25 gauge) was found to be 4.55 (m^2/g), which was much greater than those of the other samples. Also, a comparison of the samples revealed that the tensile strain and modulus of PEO nanofiber sheets (25 gauge) were better by 10% and a factor of 4, respec-

tively, compared to the PEO nanofiber sheets (21 gauge).

The degradation temperature of PEO nanofiber sheets (25 gauge) increased slightly compared to the other electrospun sample (21 gauge) and PEO nanofiber sheets with high surface area were confirmed to improve thermal stability. Oil treatment caused the opacity of PEO nanofiber sheets to decrease slightly compared to products A and B, for which the change in transparency was influenced by their original color. The oil absorption of the PEO nanofiber sheets are about 11 times greater than those of commercial products. The PEO nanofiber sheets (25 gauge) proved to offer superior oil blotting performance relative to the (21 gauge) sheets, because of the higher surface area. These results point to the promise of application of these materials in both the cosmetic and industrial fields through ongoing research.

Acknowledgements: This research was supported by the Basic Science Research Program through the National Research Foundation of Korea (NRF) under the auspices of the Ministry of Education (Grant No. 2009-0093817 and 2015 R1C1A2A01056280).

References

1. C. P. Karan, R. S. Rengasamy, and D. Das, *Indian J. Fibre Text. Res.*, **36**, 190 (2011).
2. H. Li, W. Wu, M. M. Bubakir, H. Chen, X. Zhong, Z. Liu, Y. Ding, and W. Yang, *J. Appl. Polym. Sci.*, **131**, 1 (2014).
3. K. Sudesh, C.-Y. Loo, L.-K. Goh, T. Iwata, and M. Maeda, *Macromol. Biosci.*, **7**, 1199 (2007).
4. F. Yuan, J.-F. Wei, E. Q. Tang, and K. Zhao, *e-Polymers*, **9**, 1 (2009).
5. E.-S. Jang, W.-K. Lee, C.-Y. Park, S.-K. Min, and S.-H. Jang, *J. Environ. Sci. Int.*, **22**, 243 (2013).
6. J. Lin, B. Ding, J. Yang, J. Yu, and G. Sun, *Nanoscale*, **4**, 176 (2012).
7. S. Mahajan, S. Renker, P. F. W. Simon, J. S. Gutmann, A. Jain, S. M. Gruner, L. J. Fetters, and G. W. Coates, *Macromol. Chem. Phys.*, **204**, 1047 (2013).
8. T. S. Bailey, C. M. Hardy, T. H. Epps, and F. S. Bates, *Macromol.*, **35**, 7007 (2002).
9. S. Angot, D. Taton, and Y. Gnanou, *Macromol.*, **33**, 5410 (2000).
10. M. A. Hillmyer and F. S. Bates, *Macromol.*, **29**, 6994 (1996).
11. D.-T. Caroline, P. Cosette, G. Molle, G. Muller, and E. Dé, *Protein Science*, **12**, 681 (2003).
12. J. Gustafsson, H. Ljusberg-Wahren, M. Almgren, and K. Larsson, *Langmuir*, **13**, 6964 (1997).
13. J. Hu, Y. Qian, X. Wang, T. Liu, and S. Liu, *Langmuir*, **28**, 2073 (2012).
14. R. Y. Lochhead, *The role of polymers in cosmetics: recent trends*, ACS Symposium Series, American Chemistry Society, 1996, Vol **961**, pp 3-56 (1996).
15. J. N. Israelachvili, *Proc. Natl. Acad. Sci. U.S.A.*, **94**, 8378 (1997).
16. E. Calabrò and S. Magazù, *Adv. Phys. Chem.*, **2013**, 1 (2013).
17. M. K. Pilehrood, M. Dilamian, M. Mirian, H. Sadeghi-Aliabadi, L. Maleknia, P. Nousiainen, and A. Harlin, *BioMed. Res. Int.*, **2014**, 1 (2014).
18. V. A. Liu, W. E. Jastromb, and S. N. Bhatia, *J. Biomed. Mater. Res.*, **60**, 126 (2002).
19. A. Rösler, G. W. M. Vandermeulen, and H.-A. Klok, *Adv. Drug Deliv. Rev.*, **64**, 270 (2012).
20. A. A. Azli, N. S. A. Manan, and M. F. Z. Kadir, *Adv. Mater. Sci. Eng.*, **2015**, 1 (2015).
21. S. C. Moon, B.-Y. Ryu, J. K. Cho, B. W. Jo, and R. J. Farris, *Polym. Eng. Sci.*, **49**, 52 (2009).
22. N. Gondaliya, D. K. Kanchan, P. Sharma, and P. Joge, *Adv. Mater. Sci. Appl.*, **2**, 1639 (2011).